Mesoscopic Transport in Tunable Andreev Interferometers

P. G. N. de Vegvar, T. A. Fulton, W. H. Mallison, and R. E. Miller
AT&T Bell Laboratories, Murray Hill, New Jersey 07974
(Received 29 March 1994; revised manuscript received 7 July 1994)

Low temperature transport measurements have been performed on nanofabricated Au wires a few μm long contacting two Nb electrodes whose superconducting phase difference $\Delta\theta$ was externally controlled. $\Delta\theta$ was generated by passing a known supercurrent through a series array of 28 Nb-AlO_x-Nb Josephson junctions. The conductance of the Au wire displays a component in $\Delta\theta$ with period 2π. These conductance oscillations arise from the change in scattering boundary conditions of quasiparticles in the Au wire at the Au-Nb interfaces due to Andreev reflection.

PACS numbers: 74.50.+r, 73.50.Jt, 74.80.Fp

When the size of a normal conducting system approaches the phase-breaking length L_ϕ, the low frequency linear electronic transport can be pictured in terms of transmission coefficients arising form interfering path [1,2]. Elastic scattering at the interfaces delineating the sample can then play a major role in the resulting mesoscopic phenomena. It has been proposed that superconducting-normal (SN) interfaces might offer an attractive approach to adjusting the scattering phases at surfaces [3]. In particular, the resistance R of a normal wire of length L spanning two superconductors (an SNS structure) was predicted to be sensitive to the passes imposed at the SN boundaries when $\xi_N < L < L_\phi$. According to conventional proximity effect theory, the Cooper pair amplitude decays exponentially with distance into a normal metal having electron diffusion constant D over the characteristic distance $\xi_N = (\hbar D/2\pi k_B T)^{1/2}$ [3,4]. Under these conditions the electrons and holes retain phase memory as they diffuse inside the normal wire possessing $R > 0$ while there is simultaneously negligible Josephson coupling between the two superconductors. This situation differs form the conventional SNS Josephson junction case where $L \lesssim \xi_N$ [5]. In this Letter we report on low temperature transport measurements performed using SNS devices fabricated to enter this new physical regime. By externally tuning the superconducting phase difference $\Delta\theta$ between these superconductors we find that the resistance of the normal system R varies with $\Delta\theta$ periodically. These experiments demonstrate that SN interfaces can be used to twist transmission *by acting only at the boundaries of the N system.* From a theoretical point of view, such devices directly implement the Thouless notion of resistance [6] as a rigidity modulus of the transport electrons with respect to variations in boundary conditions.

Figure 1 shows a schematic of the devices. Two Nb electrodes are spanned by a Au wire, whose resistance R is measured using four Au leads. The Nb electrodes are also connected together by a series array of N superconducting-insulating-superconducting (SIS) Josephson junctions, shunting the Au wire. The junction array established a well defined superconducting phase difference $\Delta\theta$ between the Nb electrodes contacting the Au wire. This exploits the dc Josephson relation fro a single macroscopic junction: $I_S = I_c \sin\Delta\theta$, where I_S is the supercurrent through the junction in the zero voltage state, and I_c the critical current [7]. When N such junctions are connected in series, $\Delta\theta$ accumulates across the array, giving a total phase drop $\Delta\theta = \sum_{i=1}^{N} \sin^{-1}(I_S/I_{ci})$ (I_{ci} the critical current of the ith junction). These I_{ci} are experimentally determined from the I-V curve of the junction array. All of I_S passes through the array because the Au wire has a finite resistance in the absence of Josephson coupling through it. In zero magnetic field an externally injected I_S generates a known $\Delta\theta$ between the ends of the Au wire. Having $N > 1$ junctions allows one to impose several 2π cycles of $\Delta\theta$, while $N = 1$ restricts $\Delta\theta$ to only half a period since $|I_S| < I_c$.

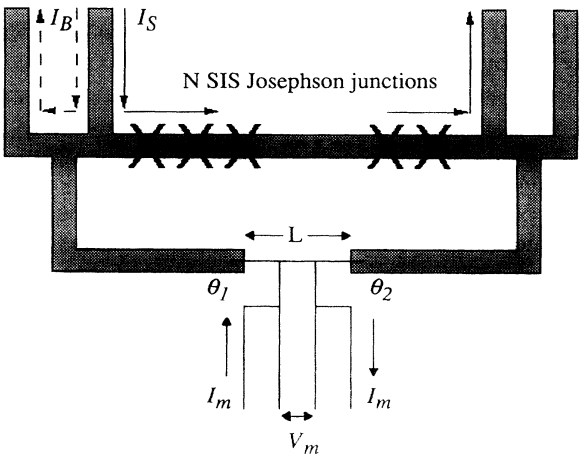

FIG. 1. A schematic of a series array of N conventional SIS Josephson junctions used to establish a known $\Delta\theta = \theta_2 - \theta_1$ between superconducting contacts to a normal Au wire. The shaded areas represent superconductors. In the devices L ranges from 4 to 6 μm. The Au leads used to inject an ac measuring current I_m and detect the resulting voltage response V_m are indicated. The solid and dashed curves show how supercurrents I_S and I_B are passed through the superconducting sections of the device, corresponding to the $\Delta\theta$ measurement and the heating control, respectively.

0031-9007/94/73(10)/1416(4)$06.00

These devices used an array of $N = 28$ SIS Josephson junctions with area $2 \times 2\ \mu m^2$, implemented in a Nb-AlO_x-Nb system with a superconducting $T_c \approx 9.1$ K. these materials were chosen to maximize the fraction α of Andreev scattering through their closely matched Fermi velocities (within 2.2%) and high T_c/T. To reduce the effect of residual uniform magnetic field on $\Delta\theta$ we arranged the junctions to be in a gradiometer configuration. The Au wires were fabricated using e-beam lithography and a liftoff process to define 28 devices and alignment marks on a Si wafer with a thermally grown oxide layer. The resulting wire widths and thicknesses ranges over 500–700 Å. The wafer was then oxygen plasma cleaned, and a trilayer consisting of Nb-AlO_x-Nb was magnetron sputter deposited after a light *in situ* Ar ion mill to establish a fresh Au surface. The junctions were fabricated from the trilayer using the selective Nb anodization process (SNAP) [8] by photolithography, reactive ion etching, and wet etching steps.

Standard ac resistance measurements as a function of I_S were performed with measuring currents I_m below 7 μA rms in a Mumetal shielded dilution refrigerator that limited stray magnetic fields to below 5×10^{-7} T. The four leads used to characterize the junction array included interference filters to reduce the coupling of extrinsic noise [9]. Typical junction I_c values ranged over 50–500 μA at 4.2 K. L_ϕ was determined from the conductance fluctuation correlation field H_c [10].

Figure 2(a) exhibits a typical low temperature $\Delta\theta$ dependence of the change in dimensionless conductance $\Delta g(\Delta\theta) = -(h/e^2)R^{-2}[\Delta V_m(I_S)/I_m]$ for sample A (S_A), where $\Delta V_m(I_S)$ is the change in the voltage response of the Au wire to the injected constant amplitude ac I_m. A slow time varying I_S was passed through the array, maintaining quasistatic experimental conditions, $\dot{\theta}L^2/D \ll 1$ and $\hbar\dot{\theta}/2e \ll \Delta V_m(I_S)$. The voltage drop across the junction array was monitored throughout the measurements to confirm that all the junctions remained in the zero-voltage state. The range of accessible $\Delta\theta$, however, was limited by the lowest critical current in the array. A correction for a small amount of Joule heating (conservatively, $\Delta T/T < 0.1$) produced by I_S passing through normal section of the feeder leads to the array has been applied. [A reproducible nonoscillatory background $g_B(I_S)$, consisting of the same injected current I_S but bypassing the junctions, was subtracted from $g(I_S)$ obtained from forcing I_S through the junctions; see Fig. 1.] The data display a reproducible oscillation, producing a corresponding peak in the Fourier transform shown in the inset.

Several control experiments were performed on S_A. Consecutive measurements confirmed a reproducibility higher than 90%. Upon warming to 4.2 K the oscillatory component vanished. Applying and removing a magnetic field of about 10^{-2} T is expected to irreversibly alter the I_{ci} by trapping flux in the array. This changes the $\Delta\theta$ vs I_S relationship. After such a field cycling we found Δg possessed the same $\Delta\theta$ periodicity even though the I_{ci} were transformed. Finally, a similar $L = 6\ \mu$m sample

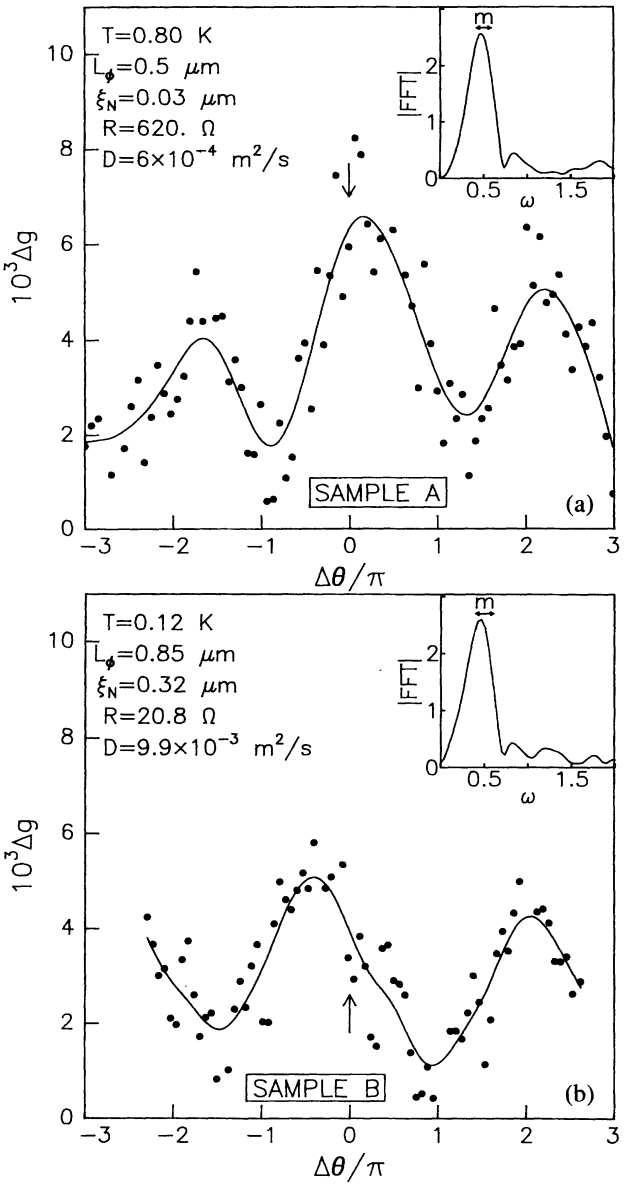

FIG. 2. The dimensionless conductance change $\Delta g(\Delta\theta)$ as measured in $L = 4\ \mu$m devices over a Au wire of length $L_w \simeq 2.9\ \mu$m. (a) Sample A, (b) sample B. Solid symbols are raw data, and the solid curves are smooth spline fits. In sample A (B) the measured segment is part of (distinct from) the Au wire bridging the superconductors. Note the different phases of the oscillations in samples A and B indicated by the vertical arrows at $\Delta\theta = 0$. Insets: Fourier amplitude spectra of the corresponding data (vertical axes in arbitrary units). ω is Fourier conjugate to $\Delta\theta/\pi$. The horizontal arrows indicate the experimental ω resolution centered at the expected $\omega = 0.5$ for mesoscopic oscillations (m) arising from two Andreev reflections occurring per round trip.

did not produce oscillations at any temperature down to 20 mK. As explained later, this mesoscopic signal should decay when $2L \gg L_\phi(T)$.

Figure 2(b) shows the measurements on sample B (S_B). S_B was fabricated independently from S_A. Because of its all superconducting array feeder leads it produced no Joule heating from I_S down to 25 mK. A similar $R(\Delta\theta)$ behavior is apparent, although with a different phase from S_A.

To interpret these observations we consider the physical processes occurring at the SN interfaces in the devices. At an SN boundary there are two mechanisms for reflecting a quasiparticle incident from the N side. One is normal reflection, and the other one is Andreev reflection [11,12] where an incoming electron (hole) is reflected as a hole (electron) and simultaneously acquired a phase shift equal to (minus) the phase of the superconducting order parameter Ψ. This Andreev process affects the measured resistance through the interlead transmission coefficients, which are constructed from interfering Feynman paths. Figure 3 shows a pair of normal leads (1,2) connected by two sorts of paths (a) and (b). In (a), an electron simply diffuses directly from 1 to 2. In (b) an electron propagates from lead 1 to superconductor S_1 having order parameter phase θ_1; there it undergoes Andreev reflection into a hole and acquires a phase shift θ_1. After diffusing to the other superconductor S_2 the hole in Andreev reflected back into an electron and absorbs a phase shift $-\theta_2$. So when the electron finally gets to lead 2 it has accumulated a total phase depending on $\Delta\theta = \theta_2 - \theta_1$. The interference path (a) and (b) arriving at lead 2 then varies with $\Delta\theta$ and, as predicted by Altshuler and Spivak (AS) [3], so does $R = R(\Delta\theta)$. In this nonensemble averaged regime, a multiprobe $R(\Delta\theta)$ should be 2π periodic with a sample dependent phase [10]. The corresponding Fourier frequency ω conjugate to $\Delta\theta/\pi$ is 0.5. Figure 2 shows clear demonstrations of this effect. There are similar contributions to $R(\Delta\theta)$ involving path (b) interfering with its time reversed conjugate that survive ensemble averaging like weak localization effects [13]. These have a period $\Delta\theta = \pi$ with an associated $\omega = 1$. As seen from the insets to Fig. 2 there is ample Fourier power in at $\omega = 0.5$, but the response at $\omega = 1$, requiring two phase-coherent round trips, lies in the noise.

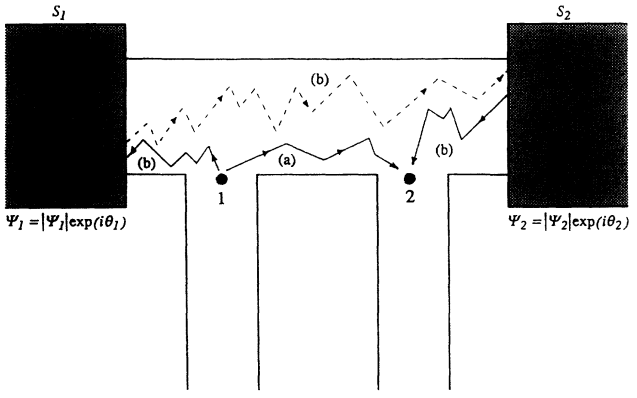

FIG. 3. Two kinds of Feynman paths contributing to the transmission coefficient between leads 1 and 2 of a normal mesoscopic system contacting two superconducting electrodes S_1 and S_2 in the regime where $\xi_N < L \lesssim L_\phi$. Path (a) represents diffusion directly from 1 to 2. Path (b) shows the electron (solid line) Andreev reflected as a hole (dashed line) at one SN interface, and then back into an electron at the other one.

Several features of the data substantiate this mesoscopic picture. First, such a mechanism should yield a $R(\Delta\theta)$ oscillation having a sample dependent phase, as is observed. This is in contrast to any other hypothetical mechanism related to the proximity effect, which is not expected to exhibit sample-to-sample variations. The measured amplitude can also be compared to mesoscopic theory. AS [Ref. [3], Eq. (11)] predict the rms dimensionless conductance amplitude as $\delta g^2 \simeq (E_c/k_BT)\exp[-L_C/L_\phi]$, where L_C is the device dependent path length over which electrons and holes need to travel phase coherently and E_c is the correlation energy. We find for S_A the ratio of experimental to theoretical amplitudes is 1.6, and for S_B it is 1.1 [14]. Similar calculations establish that the 2π periodic signal should lie beneath the measurement noise floor for the $L = 6$ μm sample and also account for the absence of π periodic ($\omega = 1$) signals.

Figure 4 presents the temperature dependence of the oscillation amplitude in S_B. The phase of the oscillations does not vary with T. This is expected for a mesoscopic mechanism in S_B since energy averaging occurs there over

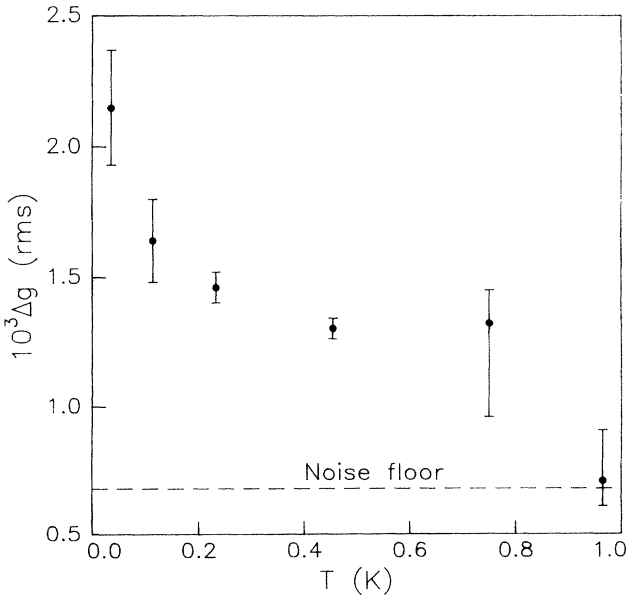

FIG. 4. Temperature dependence of the rms dimensionless conductance amplitude for sample B. The error bars indicate the measurement reproducibility.

only $k_BT/E_c \approx 1$ levels for $T \lesssim 1.0$ K [14]. If we use the above AS formula to extract an L_ϕ given the observed δg, then the data shown in Fig. 4 can be accounted for by an inferred $L_\phi(T)$ that shrinks 15% as T rises from 36 mK to 0.97 K. This weak temperature variation of L_ϕ below 1 K agrees with the work of Peters, Bergmann, and Mueller [15] on Au films. However, it is at variance with the measurements of Echternach *et al.* [16] on arrays of long Au wires that imply a larger change in L_ϕ. Perhaps the time reversal symmetry breaking imposed by $\Delta\theta \neq 0$ is playing a role here.

There is a mathematical isomorphism between the $R(\Delta\theta)$ experiments discussed here and the Aharonov-Bohm (AB) effect in an annulus where R depends on the magnetic flux Φ through the hole [10] according to $\Delta\theta \rightarrow 2\pi\Phi/\Phi_0$, where $\Phi_0 = h/e$. Physically, however, they are distinct. In the Andreev interferometer one externally controls the phase change experienced by electrons as they scatter off an interface. In the AB effect the interference occurs as an electron travels in the two branches of the ring, thereby coupling its orbital motion to the vector potential generated by Φ. Both mechanisms alter the interlead transmission probabilities.

In our experiments a known superconducting $\Delta\theta$ is *directly* applied across the Au wire in the absence of a magnetic field. This differs significantly from the magnetoresistance experiments of Petrashov *et al.* [17] on Ag mesoscopic systems in contact with superconducting Al "mirrors." Those devices were arranged as physically interpenetrating normal and superconducting circuits, and the results were consistent with a picture in which the superconductors had an arbitrary $\Delta\theta$ [18]. Their work was also interpreted in terms of a surprising Josephson coupling over lengths $L \gg \xi_N$ through Ag wires; however, our SNS devices have so far displayed no evidence for such as effect. This discrepancy could be due to the different choice of materials, interface conditions, or device configurations.

These measurements present evidence for the crucial features of externally tunable Andreev reflection interferometers. They demonstrate that it is possible to experimentally adjust scattering boundary conditions by acting only at the interfaces of mesoscopic systems, substantiating the theoretical picture of transport in SNS structures when $\xi_N < L \lesssim L_\phi$. This novel experimental technique can be directly applied to twist electronic boundary conditions in other systems, a method so far restricted to the domain of numerical simulations. It is interesting, for example, to "twist" a conductor near a metal-insulator transition to see what happens as the localization length ξ_L enters the physics. For example, one could directly examine the sensitivity of the electronic transport or dielectric constant to variations of scattering boundary conditions as L and ξ_L cross over. High T_c superconductors can also be sued to extend the temperature range of these devices, provided that the Andreev mechanism continues to operate. This technique can also be used to address the question of what happens to Andreev reflection in non-BCS superconductors.

We gratefully acknowledge the contributions of L. N. Dunkleberger and L. Smith to the sample processing.

[1] R. Landauer, IBM J. Res. Dev. **32**, 306 (1988).
[2] M. Büttiker, IBM J. Res. Dev. **32**, 317 (1988).
[3] B. Z. Spivak and D. E. Khmel'nitskii, JETP Lett. **35**, 412 (1982); B. L. Altshuler and B. Z. Spivak, Sov. Phys. JETP **65**, 343 (1987).
[4] G. Deutscher and P. G. de Gennes, in *Superconductivity*, edited by R. D. Parks (Dekker, New York, 1970) p. 1005.
[5] J. Clarke, Proc. R. Soc. London A **308**, 447 (1969); B. J. van Wees, K.-M. H. Lenssen, and C. J. P. M. Harmans, Phys. Rev. B **44**, 470 (1991).
[6] J. T. Edwards and D. J. Thouless, J. Phys. C **5**, 807 (1972).
[7] M. Tinkham, *Introduction to Superconductivity* (R. E. Krieger, New York, 1980) p. 193.
[8] H. Kroger, L. N. Smith, and D. W. Jillie, Appl. Phys. Lett. **39**, 280 (1981).
[9] T. A. Fulton and L. N. Dunkleberger, Phys. Rev. B **9**, 4760 (1974).
[10] S. Washburn, in *Mesoscopic Phenomena in Solids*, edited by B. L. Altshuler, P. A. Lee, and R. A. Webb (Elsevier, Amsterdam, 1991).
[11] A. F. Andreev, Sov. Phys. JETP **19**, 1228 (1964).
[12] G. E. Blonder, M. Tinkham, and T. M. Klapwijk, Phys. Re. B **25**, 4515 (1982).
[13] A. G. Aronov and Yu. V. Sharin, Rev. Mod. Phys. **59**, 755 (1987).
[14] Following S. Washburn and R. A. Webb, Adv. Phys. **35**, 412 (1986), Eq. (12.2), we have set $E_c/k_BT \equiv \min(2\pi\hbar D/L_\phi^2 k_B T, 1)$, giving for sample A, $10^3\delta g(0.80\text{ K}) \simeq 1.01$ (vs 1.58 observed) with a measured $L_\phi \simeq 0.5\ \mu$m, and for B, $10^3\delta g(36\text{ mK}) \simeq 1.92$ (vs 2.15 observed) with $L_\phi \simeq 0.90\ \mu$m.
[15] R. P. Peters, G. Bergmann, and R. M. Mueller, Phys. Rev. Lett. **58**, 1964 (1987).
[16] P. M. Echternach *et al.*, Phys. Rev. B **48**, 11 516 (1993).
[17] V. T. Petrashov *et al.*, Phys. Rev. Lett. **70**, 347 (1993).
[18] P. G. N. de Vegvar and L. Glazman, Phys. Rev. Lett. **71**, 2351 (1993).

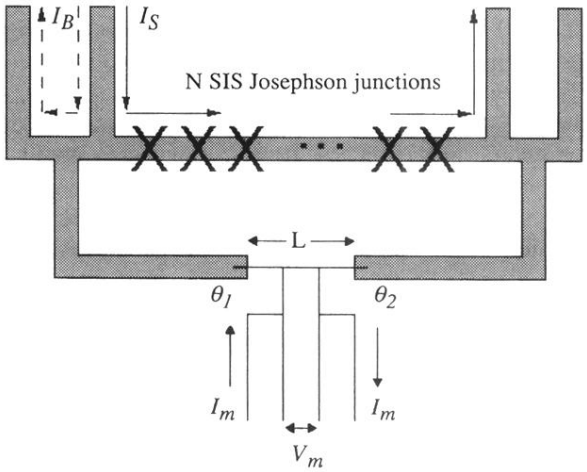

FIG. 1. A schematic of a series array of N conventional SIS Josephson junctions used to establish a known $\Delta\theta = \theta_2 - \theta_1$ between superconducting contacts to a normal Au wire. The shaded areas represent superconductors. In the devices L ranges from 4 to 6 μm. The Au leads used to inject an ac measuring current I_m and detect the resulting voltage response V_m are indicated. The solid and dashed curves show how supercurrents I_S and I_B are passed through the superconducting sections of the device, corresponding to the $\Delta\theta$ measurement and the heating control, respectively.

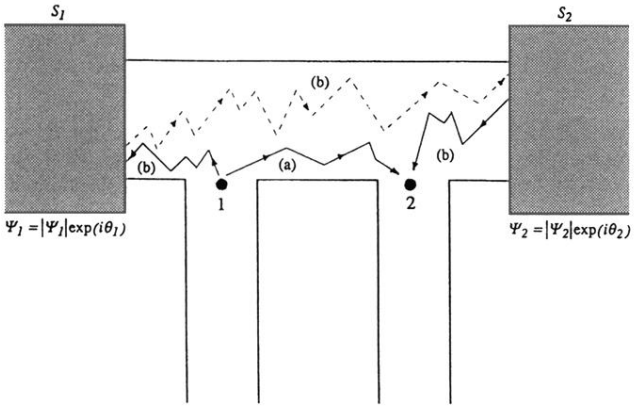

FIG. 3. Two kinds of Feynman paths contributing to the transmission coefficient between leads 1 and 2 of a normal mesoscopic system contacting two superconducting electrodes S_1 and S_2 in the regime where $\xi_N < L \lesssim L_\phi$. Path (a) represents diffusion directly from 1 to 2. Path (b) shows the electron (solid line) Andreev reflected as a hole (dashed line) at one SN interface, and then back into an electron at the other one.